Generation and Characterization of Diphosphene and Triphosphene Radical Anions. Computational Studies on the Structure and Stability of $P_3H_3^{\bullet-}$ †

Herbert Binder,* Bernhard Riegel, Gernot Heckmann, Michael Moscherosch, and Wolfgang Kaim

Institut für Anorganische Chemie der Universität Stuttgart, Pfaffenwaldring 55, D-70569 Stuttgart, FRG

Hans-Georg von Schnering and W. Hönle

Max-Planck-Institut für Festkörperforschung, Heisenbergstrasse 1, D-70569 Stuttgart, FRG

Heinz-Jürgen Flad‡

Institut für Theoretische Chemie der Universität Stuttgart, Pfaffenwaldring 55, D-70569 Stuttgart, FRG

Andreas Savin

Laboratoire Dynamique des Interactions Moleculaires (CNRS, UPR 271),
Université Pierre et Marie Curie, Tour 22, 4 Place Jussieu, 75252 Paris, Cedex 05, France

Received May 26, 1995⊗

Complexation of the K^+ ions of little soluble $K_2[^t\text{BuP}]_2\cdot{}^1/_2\text{THF}$ (THF = tetrahydrofuran) with 18-crown-6 or [2.2.2]cryptand in THF leads to brown-red solutions which exhibit limited stability at room temperature. The ^{31}P NMR spectrum consists of two singlets (1:1) which are assigned to the *trans* and *gauche* rotamers of the dianion $[^t\text{BuP}-\text{P}^t\text{Bu}]^{2-}$. That dianion undergoes a protonation by the solvent forming the monoanion $[(^t\text{Bu})(\text{H})\text{P}-\text{P}^t\text{Bu}]^-$, which has been characterized by ^{31}P NMR spectroscopy. In addition, the brown-red solutions contain a paramagnetic species, for which the EPR spectrum revealed a 1:2:1 triplet caused by the hitherto unknown diphosphene radical anion $[^t\text{BuP}{=}\text{P}^t\text{Bu}]^{\bullet-}$ (g_{iso} = 2.0103). These reactions of the dianion $[^t\text{BuP}-\text{P}^t\text{Bu}]^{2-}$ on complexation of the K^+ ions occur also at −40 °C and can be attributed to a tendency to reduce the Coulombic repulsion between the adjacent negative charges. The homologous triphosphene radical anion $[^t\text{BuP}-(^t\text{Bu})\text{P}-\text{P}^t\text{Bu}]^{\bullet-}$ could be generated by reduction of the cyclic triphosphane $(^t\text{BuP})_3$ on a potassium mirror. The new triphosphene radical anion was identified by its EPR spectrum which showed a triplet of doublets (g_{iso} = 2.0098). Finally, reduction of the neutral valence isoelectronic cyclic diphosphirane $(CH_3)_2C(^t\text{BuP})_2$ on a potassium mirror yields the radical anion $[(CH_3)_2C(^t\text{BuP})_2]^{\bullet-}$, which exhibits a 1:2:1 triplet in the EPR spectrum (g_{iso} = 2.0060). The triphosphene radical anion $[^t\text{BuP}-(^t\text{Bu})\text{P}-\text{P}^t\text{Bu}]^{\bullet-}$ is related to the radical anions $O_3^{\bullet-}$, $S_3^{\bullet-}$ and $P_3^{\bullet4-}$, but in contrast to $O_3^{\bullet-}$ and $S_3^{\bullet-}$, the pattern of hyperfine coupling constants is "reversed". Quantum-chemical calculations of $[P_3H_3]^{\bullet-}$ suggest an open-chain structure for $[^t\text{BuP}-(^t\text{Bu})\text{P}-\text{P}^t\text{Bu}]^{\bullet-}$. A possible explanation is given for the reversion of the hyperfine coupling pattern due to the shape of the highest occupied orbital. The adiabatic electron affinities are calculated for two possible structures of $[P_3H_3]^{\bullet-}$.

Introduction

The dinegatively charged oligophosphide compounds $K_2[\text{P}^t\text{Bu}]_2$ (**1**)[1] and $K_2[\text{P}^t\text{Bu}]_4$ (**2**)[2] have frequently been used as building components for the preparation of heteropoly(cyclophosphanes). Up to now it has not been possible to obtain single crystals of **1** or **2** for structure determination. NMR data of **1** are also unknown due to its virtual insolubility, whereas **2** is slightly soluble in THF and shows an AA′XX′ spin system in the ^{31}P NMR spectrum, supporting its formulation.[4] In order to get **1** into solution to investigate its NMR spectrum, the complexation of the K^+ ions was attempted with 18-crown-6 or [2.2.2]cryptand, respectively. A brown-red solution develops spontaneously after addition of either ligand, resulting in the appearance of two singlets and an AB system in the $^{31}P\{^1H\}$ NMR spectrum. Both singlet signals disappear after a few minutes, and only the AB system is left. The appearance of the reddish brown solution caused us to further investigate the solution by EPR spectroscopy. During this investigation it was discovered that **1** forms a persistent paramagnetic species both with 18-crown-6 as well as with [2.2.2]cryptand; a 1:2:1 triplet signal was observed in the EPR spectrum which we identify as being due to $[^t\text{BuP}{=}\text{P}^t\text{Bu}]^{\bullet-}$ (**1b**). During the attempt to synthesize $K_2[\text{P}^t\text{Bu}]_3$ (**3**) from $(^t\text{BuP})_3$,[5] the connecting link between **1** and **2**, a triplet of doublets originating from a short-lived paramagnetic species with the probable composition $[^t\text{Bu}-$

† Dedicated to Professor Marianne Baudler on her 75th birthday.

‡ Present address: Max-Planck-Institut für Physik komplexer Systeme, Aussenstelle Stuttgart, Heisenbergstrasse 1, D-70569 Stuttgart, FRG.

⊗ Abstract published in *Advance ACS Abstracts,* March 1, 1996.

(1) Baudler, M. *Angew. Chem.* **1982**, *94*, 520; *Angew. Chem., Int. Ed. Engl.* **1982**, *21*, 492.
(2) Issleib, K.; Hoffmann M. *Chem. Ber.* **1966**, *99*, 1320.
(3) Cowley, A. H.; Jones, R. A.; Mardones, M. A.; Atwood, J. L.; Bott, S. G. *Angew. Chem.* **1991**, *103*, 1163; *Angew. Chem., Int. Ed. Engl.* **1991**, *30*, 1141.
(4) Baudler, M.; Gruner, C.; Fürstenberg, G.; Kloth, B.; Saykowski, F.; Özer, U.; *Z. Anorg. Allg. Chem.* **1978**, *446*, 169.

0020-1669/96/1335-2119$12.00/0

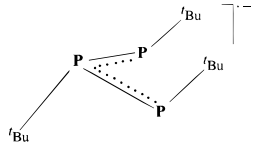

5b

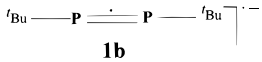

1b

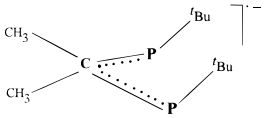

6

P−P(*t*Bu)−P*t*Bu]$^{\bullet-}$ (**5b**) was found in the EPR spectrum. The reduction of the valence isoelectronic cyclic diphosphirane $(CH_3)_2C(^t\text{BuP})_2$ resulted in the formation of the radical anion $[(CH_3)_2C(^t\text{BuP})_2]^{\bullet-}$ (**6**), which showed a triplet in the EPR spectrum. In the following we report the characterization of the ^{31}P NMR and EPR spectroscopically analyzed reaction products as well as a theoretical study of the parent ion $P_3H_3^{\bullet-}$. Considering the novelty of the system, we have studied the relative stabilities of several possible structures for the $P_3H_3^{\bullet-}$ anion using *ab initio* quantum chemistry methods. It should be mentioned that substituting the *t*Bu groups by H atoms leads to a drastical decrease of steric constraints which can shift relative stabilities. Nevertheless, we were forced to make this approximation because it allows the application of methods which lead to a reasonable description of negatively charged molecules. It is necessary to take care of electron correlation, where we have to distinguish between near degeneracy and dynamic contributions. To get a well-balanced description of both parts, we have chosen for our final calculations the multireference configuration interaction (MRCI) method. Near degeneracy is well-described by a complete active space self-consistent field (CASSCF) wave function, which contains all possible configurations that can be generated from a given set of active orbitals. We have used CASSCF wave functions to optimize the structures of the anions. For each detected minimum, extensive configuration interaction (SDCI) calculations were carried out by taking into account single and double excitations from the dominant configuration state function (CSF) of the CASSCF wave function. In order to test the basis set dependence of our results, we have used several types of basis sets for these calculations. Finally, we have carried out MRCI calculations for selected structures and basis sets.

Experimental Section

Phosphorus-31 NMR spectra {$\delta(H_3PO_4, 85\%) = 0.00$ ppm} were obtained on a Bruker AM 200 NMR spectrometer operating at 81.015 MHz.

EPR spectra were recorded in the X-band with a Bruker spectrometer ESP 300. The *g* factors were determined with the aid of a Hewlett-Packard frequency counter 5350 B and a Bruker NMR Gaussmeter ER 035 M. The di- and triphosphene radical anions were generated *in situ* in toluene under an argon atmosphere.

[*t*BuP═P*t*Bu]$^{\bullet-}$ (1b). A few milligrams of [2.2.2]cryptand were added to a suspension of $K_2[P^t\text{Bu}]_2 \cdot {}^1/_2\text{THF}$ (THF = tetrahydrofuran) in toluene in an EPR capillary tube, during which the reddish brown radical anion **1b** was formed. The solution was investigated EPR spectroscopically at room temperature. To determine the *g* anisotropy, a freshly prepared solution of the radical anion was quickly frozen in liquid nitrogen and the glassy frozen solution was examined at 120 K.

[*t*BuP(P*t*Bu)$_2$]$^{\bullet-}$ (5b). In dilute toluene solution, colorless tri-*tert*-butylcyclophosphane[5] $(P^t\text{Bu})_3$ was reduced to the reddish brown radical anion **5b** in the presence of [2.2.2]cryptand on a potassium mirror and was studied EPR spectroscopically at 293 K. Alternatively, potassium naphthalide can be used as a reducing agent; however, the signals of unreacted naphthalide radical anion disturb the spectrum of **5b**.

[(CH$_3$)$_2$C(P*t*Bu)$_2$]$^{\bullet-}$ (6). In dilute toluene solution, colorless 1,2-di-*tert*-butyl-3,3-dimethyl-1,2-diphosphacyclopropane[6] was reduced to the brown radical anion **6** in the presence of [2.2.2]cryptand on a potassium mirror.

Table 1. NMR Data of **4a** und **4b**

	δ [ppm]	^nJ [Hz]	
	Compound **4a**		
$^{31}P_A$	−1.8	$^1J(^{31}P_A{}^1H)$	197.9
$^{31}P_B$	−50.9	$^2J(^{31}P_B{}^1H)$	27.5
^1H	4.3	$^3J(^{31}P_A{}^1H)$	10.9
$^1H(^t\text{BuP}_A)$	1.59	$^3J(^{31}P_B{}^1H)$	9.5
$^1H(^t\text{BuP}_B)$	1.87	$^1J(^{31}P_A{}^{31}P_B)$	318.5
	Compound **4b**		
$^{31}P_A$	−3.9	$^1J(^{31}P_A{}^{31}P_B)$	318.0
$^{31}P_B$	−50.5	$^1J(^{31}P_A{}^2D)$	29.9

Results and Discussion

Properties of the Dianion [*t*BuP−P*t*Bu]$^{2-}$ and Characterization of the Di-*tert*-butyldiphosphene Radical Anion [*t*BuP═P*t*Bu]$^{\bullet-}$ (1b). The potassium salt $K_2[^t\text{BuP}]_2 \cdot {}^1/_2\text{THF}$ (**1**) which is produced by cleavage of tetra-*tert*-butylcyclotetraphosphane $(^t\text{BuP})_4$ with elemental potassium is insoluble in all common solvents and could not be studied by NMR up to now. For the same reasons, it was not possible to grow single crystals for an X-ray structure analysis. Formally, **1** results from a two-electron reduction of the neutral and hitherto unknown di-*tert*-butyldiphosphene [*t*BuP═P*t*Bu]. Possibly, $K_2[^t\text{BuP}]_2 \cdot {}^1/_2\text{THF}$ (**1**) exists as a contact ion triple with partially THF-solvated K^+ ions. Both negative charges could be used to occupy a π^* orbital. According to this concept, the stabilization of the system should strongly depend on the solvatation of the potassium ions. In order to achieve solubility of **1**, we treated a suspension of **1** in THF with 18-crown-6 or [2.2.2]cryptand. In either case **1** immediately dissolved to produce a reddish brown solution. For both cases it may be assumed that a complexation of the potassium ions occurs. The new state represents a "solvent-separated" ion triple with a ''free'' dianion **1a**. The $^{31}P\{^1H\}$ NMR spectrum of a THF solution of **1** with 18-crown-6 at −40 °C shows a distinct signal at $\delta = -10.8$ ppm and a broader singlet at $\delta = -15.8$ ppm (1:1) which we ascribe to the *trans* or the *gauche* rotamers of **1a**; furthermore, an AB spin system of weak intensity is recognized at $\delta_A = -1.8$ and $\delta_B = -50.9$ ppm, respectively. With increasing temperature, the intensities of both singlets decrease irreversibly in favor of increasing intensity of the AB system which becomes the only signal present at room temperature; the singlets disappear completely. The appearance of an AB spin system [$^1J(P_AP_B) = 318.5$ Hz; see Table 1] points to a transformation of the dianion **1a**; the change of structure being probably caused by Coulombic repulsion between the adjacent negative charges which, after the complexation of the K^+ ions and perhaps a change in geometry, cannot be sufficiently stabilized. In the ^1H coupled ^{31}P NMR spectrum, part A of the AB system shows an additional doublet splitting which is caused by a newly formed P−H bond. In effect, this is then an ABX spin system which points to a monoanion $[(^t\text{Bu})(H)P_A-P_B(^t\text{Bu})]^-$ (**4a**) and which results from a protonation of **1a**. To clarify whether the H atom in **4a** originates from the solvent or from the ligand, toluene-d_8 was added before the complexation reaction. A 1:1:1 triplet [^1J(PD)], $[(^t\text{Bu})(D)P_A-P_B(^t\text{Bu})]^-$ (**4b**) was found near the P−H

(5) Baudler, M.; Hahn, J.; Dietsch, H.; Fürstenberg, G. *Z. Naturforsch.* **1976**, *B31*, 1305.

(6) Baudler, M.; Saykowski, F.; *Z. Naturforsch.* **1978**, *B33*, 1208.

Table 2. EPR Data of Radical Anions

radical anion	T (K)	a_{iso} (mT)	g factors	solvent
1b[a]	293	4.547 (2 × ^{31}P)	$g_{iso} = 2.0103$	THF or toluene
	120	$A_1 = 14.69$ (2 × ^{31}P)	$g_1 = 2.0028$	toluene
		$A_2, A_3 < 0.5$	$g_2 = 2.0061$	
			$g_3 = 2.022$	
5b[b]	293	1.242 (2 × ^{31}P)	$g_{iso} = 2.0098$	toluene
		0.574 (1 × ^{31}P)		
6[b]	293	1.410 (2 × ^{31}P)	$g_{iso} = 2.0060$	toluene
7[c,d]	293	5.63 (2 × ^{31}P)		0.1 M Bu_4NPF_6/THF
	100	$A_{\|\|} = 16.35$ (2 × ^{31}P)	$g_{\|\|} = 2.002$	0.1 M Bu_4NPF_6/THF
		$A_\perp = 0.36$ (2 × ^{31}P)	$g_\perp$ not determined	
7[b,e]	298	5.5 (2 × ^{31}P)	$g_{iso} = 2.010$	THF
8[c,f]	298	4.35 (2 × ^{31}P)	$g_{iso} = 2.0111$	0.1 M Bu_4NPF_6/DME

[a] From $K_2[P^tBu]_2$ (see text). [b] From the neutral compound by reduction with potassium. [c] From the neutral compound by electrochemical reduction. [d] Reference 7. [e] Reference 8. [f] Reference 9.

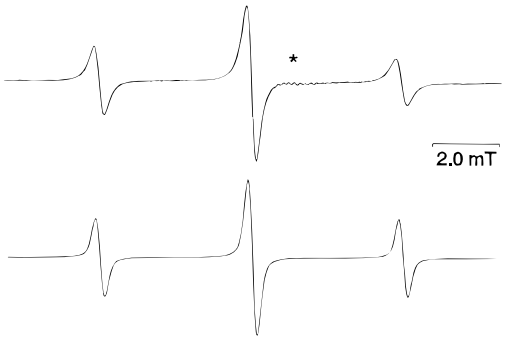

Figure 1. EPR spectrum of $[P^tBu]_2^{\bullet-}$ (**1b**, top) at 293 K in THF (*, naphthalide anion radical). Computer simulation (bottom): $a(^{31}P) = 4.547$ mT; Lorentzian line width 0.28 mT.

doublet, which clearly suggests a protonation by the solvent. By an isotopic effect, $\delta(^{31}P_A)$ in the ^{31}P NMR spectrum is shifted upfield. All NMR data of **4a** and **4b** are listed in Table 1.

It was a surprising discovery that the reddish brown solution which developed from **1** with 18-crown-6 or [2.2.2]cryptand, respectively, showed a 1:2:1 triplet in the EPR spectrum at room temperature (Figure 1); in the following, only results from the reaction with the cryptand will be reported.

The EPR triplet is caused by the coupling of one unpaired electron with two magnetically equivalent ^{31}P atoms. This result indicates the formation of the di-*tert*-butyldiphosphene radical anion, $[^tBuP{=}P^tBu]^{\bullet-}$ (**1b**), which was unknown up to now. Obviously, the very electron-rich dianion **1a** can stabilize not only by accepting a proton but also by electron transfer (oxidation), i.e., through the formation of $[^tBuP{=}P^tBu]^{\bullet-}$ (**1b**) with a three-electron π bond. The electron donating capacity of electron rich **1a** could also be demonstrated by the addition of naphthalene; the naphthalene radical anion $C_{10}H_8^{\bullet-}$ is thereby produced as evident from EPR spectroscopy.

Identification of the Tri-*tert*-butyltriphosphene Radical Anion $[^tBuP{-}(^tBu)P{-}P^tBu]^{\bullet-}$ (5b) and of $[(CH_3)_2C(^tBuP)_2]^{\bullet-}$ (6). Having characterized the di-*tert*-butyldiphosphene radical anion, we considered synthesizing a triphosphene radical anion $[RP{-}(R)P{-}PR]^{\bullet-}$. As in **1b**, a kinetic stabilization of the radical ion through the bulky ^{t}Bu groups should be possible. In fact, a radical species did develop in relatively low concentration during the reduction of $(^tBuP)_3$[5] on a potassium mirror in toluene and in the presence of [2.2.2]cryptand. The EPR spectrum showed a triplet of doublets (Figure 3). The hyperfine splitting could be caused either by an asymmetrical cyclic species $[(^tBuP)_3]^{\bullet-}$ (**5a**) or by an open-chain radical anion $[^tBuP{-}(^tBu)P{-}P^tBu]^{\bullet-}$ (**5b**) (see theoretical section). In a similiar way, we were able to generate a radical species $[(CH_3)_2C(^tBuP)_2]^{\bullet-}$ (**6**) through reduction of the corresponding three-membered heterocycle $(CH_3)_2C(^tBuP)_2$[6] on a potassium mirror and to analyze it by an EPR spectrum; **6** exhibits a 1:2:1 triplet.

Chart 1

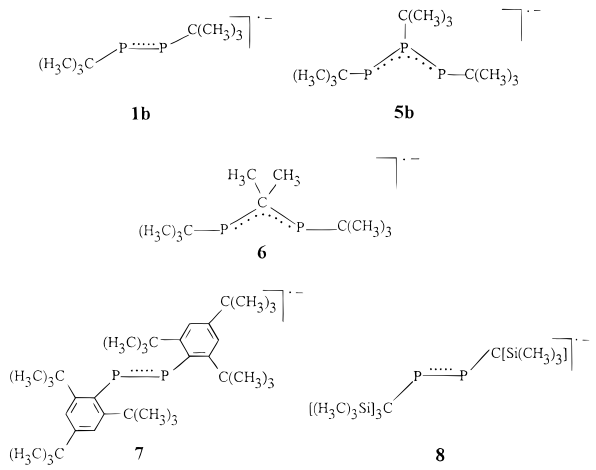

Discussion of the EPR Spectra. The EPR coupling constants and g factors of the radical anions are summarized in Table 2.

As in the solution spectra recorded for the known diphosphene radical anions **7**[7,8] and **8**[9] (Chart 1), **1b** exhibits a triplet with the intensity ratio 1:2:1 (Figure 1) which results through coupling of two magnetically equivalent ^{31}P centers ($I = {}^1/_2$) with the unpaired electron. The g factors and isotropic ^{31}P coupling constants of the diphosphene radical anions **1b**, **7**,[7,8] and **8**[9] are quite similiar (Table 1).

As observed with radical **8**,[9] the line widths of the spectrum recorded in the solution of **1b** are significantly larger on the high-field side than on the low-field side. These anisotropic line broadening effects could not be included in the simulation; however, they point to a marked anisotropy of the ^{31}P coupling as is to be expected for a planar π system. The good resolution of the EPR spectrum of **1b** in a glassy frozen solution (Figure 2) allowed us to determine the g anisotropy (rhombic symmetry) as well as one anisotropic coupling component; the other coupling constants are smaller than the observed line width of about 0.5 mT. This anisotropic ^{31}P coupling pattern confirms the π^* character of the singly occupied MO (SOMO).

The isotropic hyperfine coupling constants increase along the sequence **8** < **1b** < **7**. This correlates with the expected

(7) Geoffroy, M.; Jouaiti, A.; Terron, G.; Cattani-Lorente, M.; Ellinger, Y. *J. Phys. Chem.* **1992**, *96*, 8241.
(8) Cetinkaya, B.; Hudson, A.; Lappert, M. F.; Goldwhite, H.; *J. Chem. Soc., Chem. Commun*. **1982**, 609.
(9) Culcasi, M.; Gronchi, G.; Escudie; J.; Pujol, L.; Tordo, P. *J. Am. Chem. Soc*. **1986**, *108*, 3130.

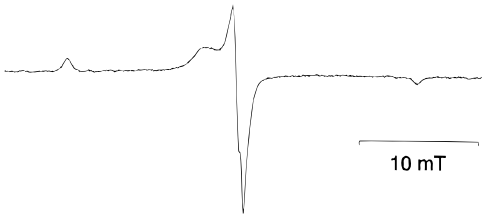

Figure 2. EPR spectrum of $[P^tBu]_2^{\bullet-}$ (**1b)** at 120 K in glassy frozen toluene solution.

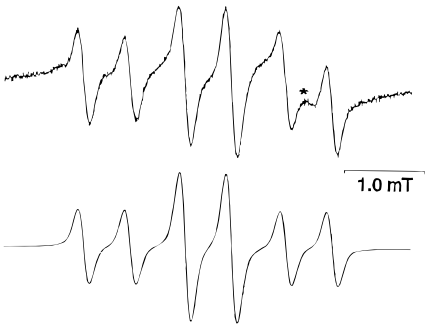

Figure 3. EPR spectrum of $[^tBuP-(^tBu)P-P^tBu]^{\bullet-}$ (**5b**, top) at 293 K in toluene (*, decomposition product). Computer simulation (bottom): $a(^{31}P) = 1.242$ mT (2P); $a(^{31}P) = 0.574$ mT (1P); Lorentzian line width 0.15 mT.

geometrical distortion at the sp^2 configurated phosphorus atoms through the sterically demanding substituents. The observed tendency can also be brought into relation with a reduction of the π character of the P−P bond, caused by the decreasing donor effect of the substituents in the order $C[Si(CH_3)_3]_3 > {}^tBu > Ar$.[10]

The radical anions **5b** and **6** were produced in low concentrations from neutral cyclic precursors by reduction with potassium. The solution spectrum of **5b** is presented in Figure 3 together with a computer simulation.

The spectrum of **5b** is a triplet of doublets consisting of six lines, as is to be expected for the coupling of two magnetically equivalent phosphorus centers and a third different ^{31}P nucleus with the unpaired electron. The spectrum of **6** shows only three lines with the intensity ratio 1:2:1. The ^{31}P coupling constant for two apparently equivalent ^{31}P nuclei in **6** is somewhat larger than that of the two equivalent centers in **5b**. On the other hand, the *g* factor of **6** is smaller due to the substitution of one RP unit by the R_2C group with light atoms only (smaller spin orbit coupling constant of C relative to P[11]).

The EPR splitting patterns of **5b** and **6** suggest that the reduction is connected to a ring opening which leads to two similar systems with magnetically equivalent terminal phosphorus centers. The spin bearing system of **5b** is isoelectronic to $S_3^{\bullet-}$,[12] possessing the same number of valence electrons (19) as the ozonide radical anion $O_3^{\bullet-}$,[13] chlorine dioxide, ClO_2, or the recently studied radical tetraanion $P_3^{\bullet 4-}$.[14] In the case of the ozonide and the trisulfide radical anions, the isotropic hyperfine coupling constants of the terminal nuclei are only half as large as those of the central atoms: $O_3^{\bullet-}$, $a(^{17}O) = 1.12$ mT (2 O), $a(^{17}O) = 2.22$ mT (1 O);[13] $S_3^{\bullet-}$, $a(^{33}S) = 0.94$ mT (2 S), $a(^{33}S) = 1.82$ mT (1 S).[12]

In contrast to these results, the larger value of $a(^{31}P)$ in radical **5b** has to be attributed to the two equivalent terminal phosphorus atoms. The reason for the "inverse" spin density distribution in **5b** is unclear; eventually it may be traced back to structural causes as, e.g., a very small P−P−P angle, *tert*-butyl-induced conformational distortion, or the possibility of a still existing interaction between the two terminal phosphorus atoms. A possible explanation is given below for the reversion of the coupling pattern, based on different symmetries of the highest occupied orbitals. Both radical anions **5b** and **6** are not very persistent and decompose within a few minutes at ambient temperatures, during which the intensity of the signals of the decomposition product (*) steadily increases; analyses of EPR spectra in frozen solution were thus not attempted.

Computational Studies on Structure and Stability of $P_3H_3^{\bullet-}$

Computational Considerations. All calculations were carried out with the program MOLPRO[15,16] of Werner and Knowles. In order to reduce the computational effort, we have used pseudopotentials for the P atoms.[17] Several Gaussian type orbital (GTO) basis sets were used throughout the calculations. On the P atom we have chosen the (4s, 4p) basis set of Poppe[18] which was augmented by two diffuse s and p functions taken from Ortiz.[19] This basis set together with various combinations (for further details see ref 19) of d and f type polarization functions[20,21] has been used in all calculations. A basis set of similar quality was selected for the H atom, where we have taken the 6-31 G basis set[22] augmented by two diffuse s functions with exponents 0.06 and 0.03,[23] together with Dunnings p and d type polarization functions.[24] The following combinations were used in our calculations:

BS1: (6s,6p,1d/6s,1p)/[4s,4p,1d/4s,1p]

BS2: (6s,6p,2d/6s,2p)/[4s,4p,2d/4s,2p]

BS3: (6s,6p,3d/6s,2p)/[4s,4p,3d/4s,2p]

BS4: (6s,6p,3d,1f/6s,2p,1d)/[4s,4p,3d,1f/4s,2p,1d]

BS5: (6s,6p,3d,1f/6s,2p,1d)/[5s,5p,3d,1f/4s,2p,1d]

Neutral Species P_3H_3. A large number of calculations on this molecule are reported in the literature.[25−31] Besides the

(10) Gerson, F. *High Resolution E.S.R. Spectroscopy*; Wiley: New York, 1970.
(11) Weil, J. A.; Bolton, J. R.; Wertz, J. E. *Electron Paramagnetic Resonance, Elementary Theory and Practical Applications;* Wiley: New York, 1994.
(12) Lunsford, J. H.; Johnson, D. P. *J. Chem. Phys.* **1973**, *58*, 2079.
(13) Schlick, S. *Phys. Chem. Lett*. **1969**, *4*, 421.
(14) von Schnering, H. G.; Hartweg, M.; Hartweg, U.; Hönle, W. *Angew. Chem*. **1989**, *101*, 98; *Angew. Chem., Int. Ed. Engl*. **1989**, *28*, 56.
(15) MOLPRO is a package of *ab initio* programs written by H.-J. Werner and P. J. Knowles, with contributions from J. Almlöf, R. D. Amos, M. J. O. Deegan, S. T. Elbert, C. Hampel, W. Meyer, K. Peterson, R. Pitzer, A. J. Stone, P. R. Taylor, P. R.
(16) Werner, H. J.; Knowles, P. J. *J. Chem. Phys*. **1985**, *82*, 5053. Knowles, P. J.; Werner, H. J. C*hem. Phys. Lett*. **1985**, *115*, **1985**, 259. Werner, H. J.; Knowles, P. J. *J. Chem. Phys*. **1988**, *89*, 5803. Knowles, P. J.; Werner, H. J. *Chem. Phys. Lett*. **1988**, *145*, 514.
(17) Igel-Mann, G.; Stoll, H.; Preuss, H. *Mol. Phys*. **1988**, *65*, 1321.
(18) Poppe, J. Private communication, 1988.
(19) Ortiz, J. V. *J. Chem. Phys*. **1987**, *86*, 308.
(20) Roos, B.; Siegbahn, P. *Theor. Chim. Acta* **1970**, *17*, 199.
(21) Frisch, M. J.; Pople, J. A.; Binkley, J. S. *J. Chem. Phys*. **1984**, *80*, 3265.
(22) Ditchfield, R.; Hehre, W. J.; Pople, J. A. *J. Chem. Phys*. **1971**, *54*, 724.
(23) Dykstra, C. E. *Ab Initio Calculation of the Structures and Properties of Molecules*; Elsevier: Amsterdam, 1988; p 144.
(24) Dunning, T. H., Jr. *J. Chem. Phys*. **1989**, *90*, 1007.
(25) Issleib, K.; Gruendler, W. *Theor. Chim. Acta* **1968**, *11*, 107.
(26) Schoeller, W. W.; Dabisch, T. *J. Chem. Soc., Dalton Trans*. **1983**, 2411.
(27) Yoshifuji, M.; Inamoto, N.; Ito, K.; Nagase, S. *Chem. Lett*. **1985**, 437.

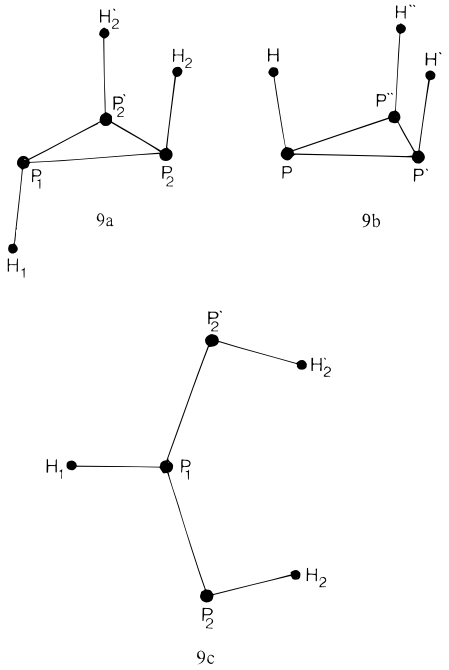

Figure 4. Structures of the neutral species P_3H_3: **9a** (*trans*), **9b** (*cis*), and **9c** (open planar).

Table 3. Calculated Bond Distances (pm) and Bond Angles (deg) for P_3H_3 (**9a**−**c**)[a]

	Structure **9a**		
$r(P_1-P_2)$	219.3	P_2-P_1-P2'	60.4
$r(P_2-P_2')$	220.6	$P_1-P_2-H_2$	95.3
$r(P_1-H_1)$	140.5	$P_2-P_2'-H_2'$	98.5
$r(P_2-H_2)$	140.5	$P_2-P_1-H_1$	95.5
	Structure **9b**		
$r(P-P')$	220.8	$P'-P-H$	98.3
$r(P-H)$	140.4		
	Structure **9c**		
$r(P_1-P_2)$	207.4	$P_2-P_1-P_2'$	142.0
$r(P_1-H_1)$	138.9	$P_1-P_2-H_2$	93.1
$r(P_2-H_2)$	140.7		

[a] The structures of **9a** and **9b** were optimized on the HF level, for **9c** we have taken the CASSCF method. Basis set BS1 has been used in all cases. For further details see Figure 4.

cyclic structures **9a** (*trans*) and **9b** (*cis*), Schoeller and Busch described the open planar structure **9c**[31] (see Figure 4). We have optimized the molecular structure for **9a** and **9b** on the Hartree−Fock [HF] level with the basis set BS1. In both cases we have assumed C_s symmetry during the optimization, whereby we obtained C_{3v} symmetry for the structure **9b**. Bond distances and angles are listed in Table 3.

Our results are in good agreement with the values reported in the literature (i.e., the recent results in refs 30 and 31). For the open planar molecule **9c**, we have optimized the structure on the CASSCF level using basis set BS1. This is necessary due to the occurrence of near degeneracy effects in the ground state. We have assumed C_{2v} symmetry, which can be justified in view of the vibrational analysis of Schoeller and Busch.[31] The electronic structure of **9c** is closely related to the ozone molecule O_3, where the importance of a well-balanced description of ionic and radical configurations is well-known (see, e.g., Goddard et al.[32] for a general valence bond description of the bonding in ozone). The active space is generated from five a_1, two a_2, b_1, and four b_2 orbitals (the molecule is placed in the *y*,*z* plane, where *z* is the principal symmetry axis), which represent all possible combinations of the 3s and 3p orbitals on the P atoms. The resulting bond distances and angles (Table 3) are in close agreement with the values reported by Schoeller and Busch,[31] besides the P−P bond distance for which we got 207.4 pm compared with the 203.1 pm of Schoeller and Busch. This is due to a near degeneracy effect represented by a double excitation from $(1a_2)^2 \rightarrow (2b_1)^2$. The same effect can be observed for ozone.[33] We have calculated the energy differences of the structures **9b** and **9c** with respect to the most stable structure **9a** on various levels of theory using different basis sets. The results are summarized in Table 4 and Figure 5a,b.

Table 4. Relative Stabilities of the Structures **9a**−**c** for Various Methods (Energy Differences, eV)

method[a]	HF	CAS	SD−CI	SD−CI+Q
$E_{\mathbf{9b}}-E_{\mathbf{9a}}$	0.218	0.447	0.213	0.202
$E_{\mathbf{9c}}-E_{\mathbf{9a}}$	1.476	1.010	1.443	1.332

[a] Basis set BS4 has been used in all calculations

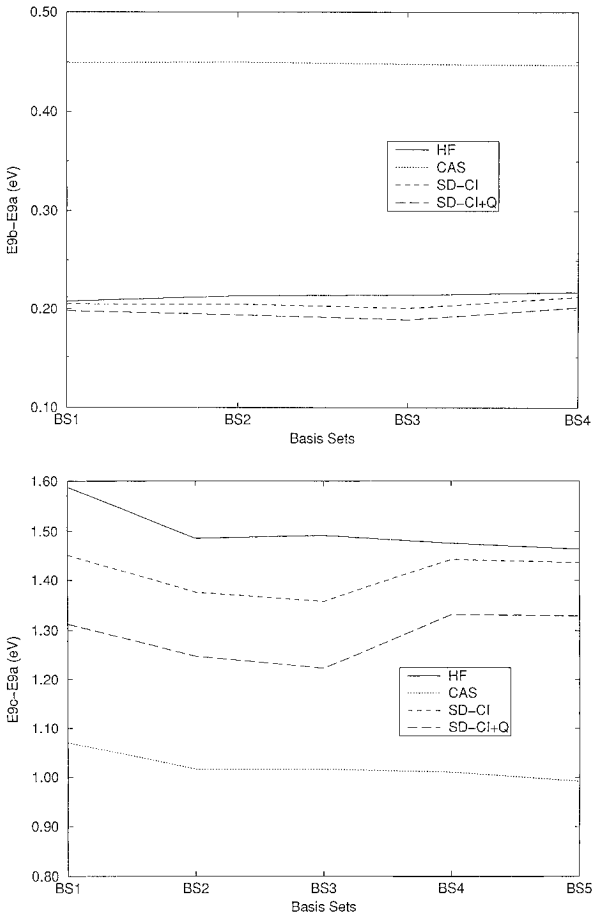

Figure 5. (a (top), b (bottom)) Basis set dependence on the relative stabilities of the structures **9a**−**c** for various computational methods.

The energy difference between **9a** and **9b** remains nearly constant at 0.2 eV in going from HF to SD−CI and SD−CI+Q, respectively (including the renormalized Davidson correction[34]); only the CASSCF results showed a significant deviation from this value. Stronger variations can be observed for the energy

(28) Gleiter, R.; Schaefer, W.; Baudler, M. *J. Am. Chem. Soc*. **1985**, *107*, 8043.
(29) Schoeller, W. W.; Staemmler, V.; Rademacher, P.; Niecke, E. *Inorg. Chem*. **1986**, *25*, 4382.
(30) Schiffer, H.; Ahlrichs, R.; Haeser, M. *Theor. Chim. Acta* **1989**, *75*, 1.
(31) Schoeller, W. W.; Busch, T. *Chem. Ber*. **1992**, *125*, 1319.
(32) Goddard, W. A., III, Dunning, T. H., Jr., T. H.; Hunt, W. J.; Hay, P. J. *Acc. Chem. Res*. **1973**, *6*, 368.
(33) Gonzalez-Luque, R.; Merchan, M.; Borowski, P.; Roos, B. O. *Theor. Chim. Acta* **1993**, *86*, 467.
(34) Langhoff, S. R.; Davidson, E. R. *Int. J. Quantum Chem*. **1974**, *8*, 61.

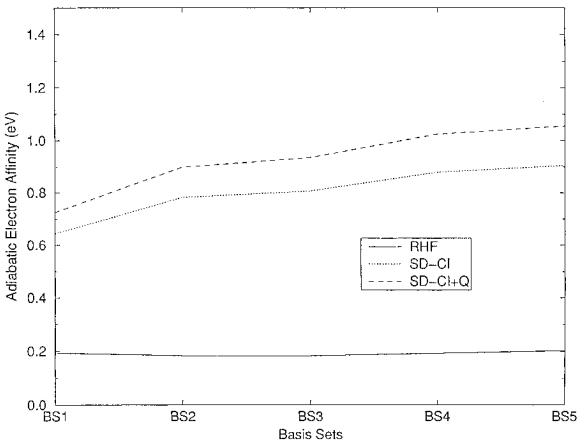

Figure 6. Adiabatic electron affinities of PH_2 for various basis sets and levels of correlation. The structures were optimized for basis set BS1 using the RHF method. Bond distances of 140.8 and 142.2 pm and angles of 93.8 and 93.7° were found for PH_2 and PH_2^-, respectively.

difference between **9a** and **9c**; in going from HF to SD−CI and SD−CI+Q we found an increase of stability for structure **9c**. The difference is still smaller on the CASSCF level, where we have an optimal description of the near degeneracy effects which are important in the case of **9c**. Nevertheless the relative order of stability for the structures **9a**−**c** remains the same on all levels of calculation. Improvements of the basis set have only little effects on the relative stabilities. The most significant changes can be observed by adding a second d and p respectively polarization function and polarization functions with higher angular momentum of f and d respectively type on P and H. Reducing the contraction of the basis set or adding a third d function on P leads only to imperceptible shifts in the relative stabilities.

Preliminary Studies on Related Systems. Studies on the electron affinity of several related systems are reported in the literature (see, e.g., refs 19, 35 and 36] for comparative studies with respect to basis sets and methods). Most of the work has been done on PH_2 and PH_2^-, where an experimental value for the electron affinity exists. We have calculated the adiabatic electron affinity (AEA) of PH_2 in order to test our basis sets on the restricted Hartree−Fock (RHF) and SD−CI level, respectively. The results are shown in Figure 6, where we have neglected the small zero-point energy contribution.

Applying Davidson's correction[34] for higher excitations (SD−CI+Q) on the SD−CI level, our results are in close agreement with pertubation theory calculations of Ortiz,[19,35] and Nguyen.[36] We have obtained an AEA of 1.077 eV for basis set BS5, taking into account the zero-point energy contributions of Nguyen[36] compared with the experimental value of 1.271 eV.[37] Another system that has been studied in the literature is the $P_2H_2^-$ anion.[38,39] In all of these cases the electron affinity is underestimated in the calculations. This should be kept in mind by the interpretation of calculated electron affinities.

Possible Structures of $P_3H_3^{\bullet-}$. Before we shall discuss several proposals for the possible structure of $P_3H_3^{\bullet-}$, one should bear in mind that aside from computational inaccuracies like incomplete basis sets and restrictions in the treatment of electron correlation, we have replaced the ^{t}Bu groups by H atoms. As already mentioned, this can lead to significant shifts in the relative stabilities for various arrangements of these groups on the phosphorus skeleton due to steric repulsion. Unfortunately we can discuss these effects only in a rather crude and qualitative fashion because of the computational effort which increases drastically in going from H to ^{t}Bu groups. Experimental results strongly indicate a regular distribution of the H atoms on the three P atoms. We have found two energetically very close open structures **10a** and **10b** (Figure 7) which belong to different electronic states (^{2}A′ and ^{2}A″, respectively).

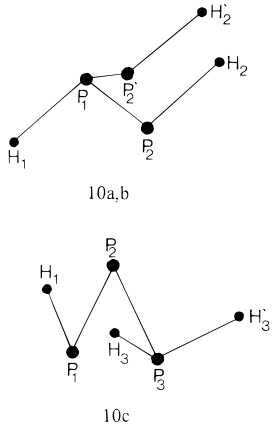

Figure 7. Possible structures of $P_3H_3^{\bullet-}$: two energetically very close open structures **10a** and **10b**, which belong to different electronic states (^{2}A′ and ^{2}A″, respectively), and **10c**, where a H atom is moved from the central to an outer position.

Table 5. Calculated Bond Distances (pm) and Bond Angles (deg) for Various Structures of $P_3H_3^{\bullet-}$ (**10a**−c)[a]

Structure **10a**, C_s Symmetry, Electronic State ^{2}A′			
$r(P_1-P_2)$	219.1	$P_2-P_1-P_2'$	129.6
$r(P_1-H_1)$	140.2	$P_1-P_2-H_2$	94.0
$r(P_2-H_2)$	141.4	$P_2-P_1-H_1$	99.6
		$H_1-P_1-P_2'-H_2'$[b]	183.3
Structure **10b**, C_s Symmetry, Electronic State ^{2}A″			
$r(P_1-P_2)$	224.2	$P_2-P_1-P_2'$	93.4
$r(P_1-H_1)$	140.9	$P_1-P_2-H_2$	93.3
$r(P_2-H_2)$	141.5	$P_2-P_1-H_1$	95.5
		$H_1-P_1-P_2'-H_2'$[b]	171.3
Structure **10c**, C_s Symmetry, Electronic State ^{2}A″			
$r(P_1-P_2)$	211.9	$P_1-P_2-P_3$	98.1
$r(P_2-P_3)$	220.7	$P_2-P_1-H_1$	94.5
$r(P_1-H_1)$	141.7	$P_2-P_3-H_3$	100.8
$r(P_3-H_3)$	141.2	$H_3-P_3-H_3'$	93.6

[a] Structures **10a** and **10b** were optimized on the CASSCF level taking the 3s and 3p orbitals of the P atoms in the active space; **10c** was optimized using the RHF method. Basis set BS1 has been used in all cases. For further details see Figure 7. [b] Viewed along the P_1-P_2' bond, the angle is traced in the clockwise sense.

Both structures were optimized on the CASSCF level, taking the same active space as described above, bond distances and angles are listed in Table 5. The most significant structural difference has been found for the P−P−P angle, which is 129.6° for **10a** and 93.4° for **10b**. Another peculiar feature is the difference in the P−P bond distance, where we have found 219.1 and 224.2 pm respectively for **10a** and **10b**. This can be explained by looking at the single occupied orbital in both cases, which belongs to a′ for **10a** and to a″ for **10b**. In the case of **10a** the single occupied orbital is of bonding character with contributions from all three P atoms, whereas for **10b** only the outer P atoms contribute to the orbital which therefore has a nonbonding character.

In the case of a RHF wave function, the spin density is equal to the orbital density of the single occupied orbital. For a quantitative description of the spin density distribution this is a quite poor approximation, but for a qualitative dicussion it is

(35) Ortiz, J. V. *Chem. Phys. Lett.* **1987**, *136*, 387.
(36) Nguyen, M. T. *J. Mol. Struct. (THEOCHEM)* **1988**, *180*, 23.
(37) Zittel, P. F.; Lineberger, W. C. *J. Chem. Phys.* **1976**, *65*, 1236.
(38) Nguyen, M. T. *J. Phys. Chem.* **1987**, *91*, 2679.
(39) Geoffroy, M.; Jouaiti, A.; Terron, G.; Cattani-Lorente, M. *J. Phys. Chem.* **1992**, *96*, 8241.

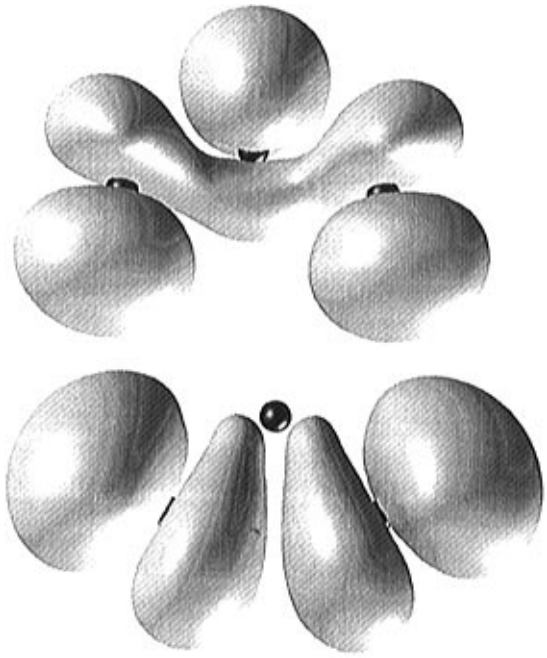

Figure 8. (a (top), b (bottom)) Isosurfaces of the orbital densities of the single occupied orbitals of structures **10a** and **10b**, respectively.

sufficient. We have plotted isosurfaces of the orbital densities in Figure 8, which approximate the spin density in both states.

Figure 8 shows the spin density of **10a** in the $^2A'$ state. It can be clearly seen that it is equally distributed over all three P atoms. In contrast to that, we have in the $^2A''$ state of **10b** the whole spin density concentrated on the two outer P atoms. Their nuclei have therefore a stronger coupling to the electron spin than the nucleus of the central P atom, generating the observed triplet of doublets EPR spectrum. Unfortunately the energy difference between **10a** and **10b** is rather small, as discussed below. There remains still some uncertainty in relating **10b** to experiment. The ground state of O_3^- has A′ symmetry[33] and generates, as already mentioned, a doublet of triplets EPR spectrum. This further supports our suggestion of **10b** as the observed structure in experiment.

For comparison we have also studied structure **10c** (Table 5), where a H atom is moved from the central to an outer position. This structure can be obtained from Nguyens [HP−PH]$^{\bullet-}$ (*trans*) structure,[38] which is the most stable arrangement for $P_2H_2^{\bullet-}$, by replacing a H atom through a PH_2 group. The P_1-P_2 (211.9 pm), P_2-H_1 (141.7 pm), $P_1-P_2-H_1$ (94.5°) bond distances and angles are in good agreement with the values reported in ref 38 (213.6 pm, 141.8 pm, and 95.8°, respectively).

Finally we have tried to determine the electron affinities for **10a**−**c**. To begin with, we have carried out SD−CI calculations with different basis sets discussed above. The AEA's with respect to the neutral molecule **9c** are shown in Figure 9a−c (the results for BS4 are listed in Table 6). Compound **9c** seems to be an adequate reference, because it is the only open neutral structure and posseses therefore the same number of P−P bonds as the anions.

It should be expected, that the accuracy of an energy difference between two structures increases with increasing similarity. Our computed AEA's are rather insensitive on the SD−CI level to the basis set, so that the relative order of stability does not change in going from BS1 to BS5. As can be seen from Table 6, **10b** is slightly more stable than **10a**, both seem to be less stable than **10c**. Higher order excitations, which are taken into account through the Davidson correction, slightly favor **10a**,**b** versus **10c**. Ultimately we have performed MRCI

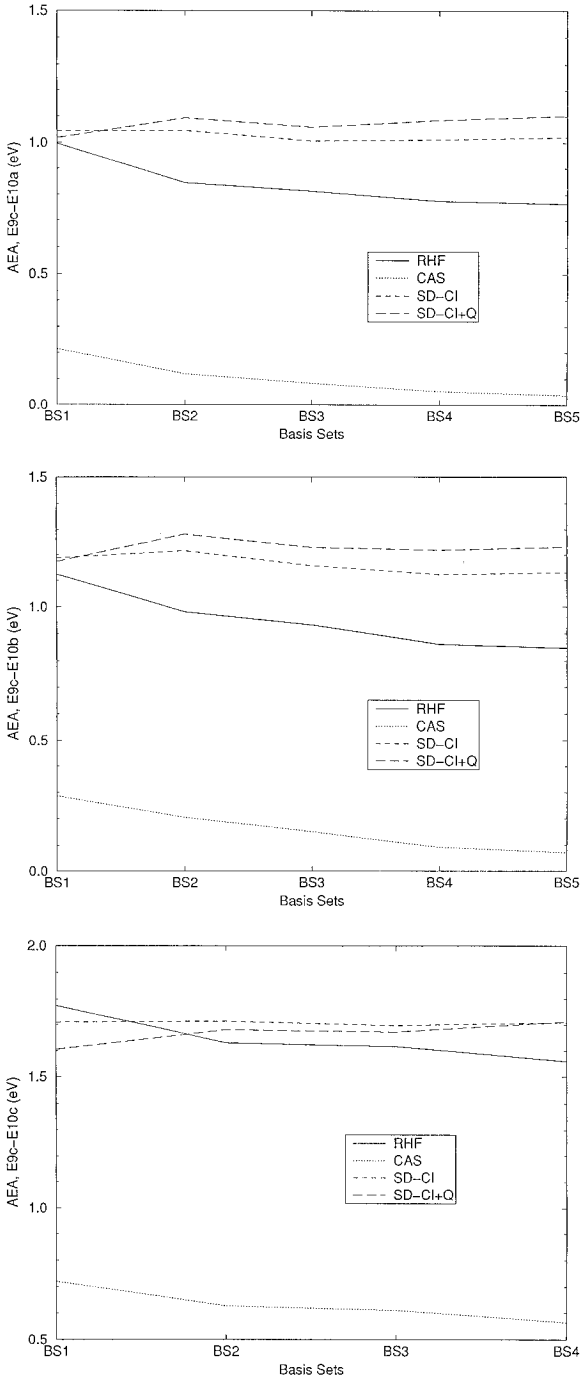

Figure 9. (a−c (from top to bottom)) Basis set dependence on the adiabatic electron affinities (AEA) of the structures **10a**−**c** with respect to the neutral structure **9c** for various computational methods.

Table 6. Adiabatic Electron Affinities (eV) for Various Levels of Correlation using Basis Set BS4 of the Anions **10a**−**c** with Respect to the Neutral Structure **9c**

method[a,b]	RHF	CAS	SD−CI	SD−CI+Q
$E_{\mathbf{9c}}-E_{\mathbf{10a}}$	0.776	0.053	1.012	1.087
$E_{\mathbf{9c}}-E_{\mathbf{10b}}$	0.861	0.093	1.124	1.220
$E_{\mathbf{9c}}-E_{\mathbf{10c}}$	1.560	0.566	1.709	1.712

[a] Basis set BS4 has been used in all calculations. [b] Zero-point energy contributions are neglected.

calculations taking the CASSCF wave function discussed above and basis set BS4. The results are listed in Table 7, together with the relative shifts compared with the SD−CI and SD−CI+Q energy differences. The relative stability of **9c** is clearly enhanced, which could be expected due to an adequate descrip-

Table 7. Results of MRCI Calculations for the Relative Stabilities and AEA (eV) of **9a**−**c**, and **10a**−**c** Together with Shifts Δ Compared with the SD−CI and SDCI+Q Energy Differences[a]

	MRCI	Δ	MRCI+Q	Δ
$E_{\mathbf{9c}}-E_{\mathbf{9a}}$	1.167	−0.276	1.179	−0.153
$E_{\mathbf{9c}}-E_{\mathbf{10a}}$	0.700	−0.312	0.965	−0.122
$E_{\mathbf{9c}}-E_{\mathbf{10b}}$	0.770	−0.354	1.054	−0.166
$E_{\mathbf{9c}}-E_{\mathbf{10c}}$	1.235	−0.474	1.494	−0.218

[a] Basis set BS4 has been used in all calculations.

tion of the bonding at the CASSCF level. On the MRCI level we observe a slight decrease in the stability of the anions **10a**−**c** relative to **9c**, but the relative order of stability remains the same.

Conclusions

The spectroscopic results strongly indicate that every P atom is associated with a ^{t}Bu group. Substituting the ^{t}Bu groups through H atoms, we have found two possible open structures **10a** and **10b** for the $P_3H_3^{\bullet-}$ anion, where the H atoms are equally distributed over the P atoms. These results have to be interpreted under the restriction that these are not the most stable arrangements for the H atoms (structure **10c** is significantly more stable). The situation may change if we replace the H atoms through ^{t}Bu groups in our calculation, which was not possible for computational reasons. When we combine two ^{t}Bu groups on a P atom, we should expect an enormous increase in the steric hindrance which can compensate for the observed energy differences between **10a**−**c**. Structures **10a** and **10b** should be nearly equivalent from the steric point of view; therefore, we would expect no significant shifts for the relative stabilities in going from H to ^{t}Bu groups. Their energy difference is rather small (approximately 0.1 eV) in all calculations, so that they can be both viewed as possible candidates for the observed anion. On the other hand, we know from the EPR spectroscopic results that the spin density is larger at the outer P atoms. As already mentioned, this excludes **10a**, leaving us with **10b** as the most probable structure.

Acknowledgment. This work was supported by the Fonds der Chemischen Industrie and the Deutsche Forschungsgemeinschaft. We are grateful to one of the reviewers for providing us with a rhombic model to interpret the frozen solution EPR spectrum of $[P_2{}^tBu_2]^{\bullet-}$.

IC950661A